Immuno-PET monitoring of CD8$^+$ T-cell infiltration post anti-ICOS agonist antibody treatment alone and in combination with PD-1 blocking antibody using an ^{89}Zr–anti-CD8$^+$ mouse minibody in EMT6 tumor-bearing mice

Poster No. 2816

Hasan Alsaid[1], Shih-Hsun Cheng[1], Meixia Bi[1], Mary Rambo[1], Tinamarie Skedzielewski[1], Bao Hoang[1], Sunish Mohanan[1], Andrew Gehman[1], Chih-Yang Hsu[1], Minh Doan[1], Fang Xie[1], Reid Groseclose[1], Christopher B Hopson[1], Sara Brett[2], Ian Wilson[3], Andrew Nicholls[2], Marc Ballas[1], Jeremy D Waight[1], Beat M Jucker[1], Axel Hoos[1]

[1]GlaxoSmithKline, Collegeville, PA, USA; [2]GlaxoSmithKline, Hertfordshire, UK; [3]ImaginAb, Inglewood, CA, USA

Background

- Inducible T-cell co-stimulator (ICOS) is a co-stimulatory receptor important for promotion of immune activation and function.[1,2]
- Despite reported clinical activity of ICOS agonism, and nonclinical studies supporting a role for ICOS in T-cell activation and proliferation, little is known regarding the potential of monoclonal antibody (mAb)-mediated ICOS co-stimulation for increasing cytotoxic T-cell infiltration into tumors.[1–7]
- Feladilimab (GSK3359609) is an immunoglobulin (Ig) G4 ICOS agonist mAb with low/no T-cell depleting potential[4] that is currently being evaluated in pivotal clinical trials.[8,9]
- Using PET/CT imaging and a rodent surrogate of feladilimab, we explored the effects of ICOS agonism on tumor CD8$^+$ T-cell infiltration alone and combined with PD-1 blockade in a subcutaneous syngeneic mouse model of breast cancer.

Methods

- A total of N=5 studies with different experimental schedules were performed (**Figure 1**).
- Female BALB/c mice with established EMT6 tumors (~150 mm^3) received 10 µg of either:
  1. ICOS agonist mAb (7E.17G9 mouse [m] IgG1) alone
  2. ICOS agonist mAb (7E.17G9 mIgG1) + PD-1 antagonist mAb (RMP1-14 rat IgG2a)
  3. Respective IgG control mAbs
- mAb treatment was given via intraperitoneal (IP) injection as per the study design (**Figure 1**).
- ^{89}Zr-labeled anti-CD8 minibody (IAB42M1-14 anti-mouse CD8 minibody, ImaginAb, CA; 10 µg, 18 µCi/µg) was given by intravenous (IV) injection and imaging of uptake in the tumor and tumor-draining lymph nodes (TDLN) was performed 24 and 48 hours (hr) post dose, per the study design (**Figure 1**).
- Immunohistochemistry (IHC) for CD8$^+$ T cells was performed at end of study.
- Imaging mass cytometry (Hyperion) was performed on tumor samples collected on Day 11 (study 4).[10] Tissue sections were stained with metal-labeled mAbs and analyzed at a pixel size of 1 µm.[10]
- 3D radiomic features were extracted from PET/CT images. Top-ranked features were used for hierarchical clustering to identify treatment effect.
- Studies were conducted in accordance with the GlaxoSmithKline (GSK) Policy on the Care, Welfare and Treatment of Laboratory Animals and were reviewed by the Institutional Animal Care and Use Committee at GSK, or by the ethical review process at the institution where work was performed.

Figure 1. Study design

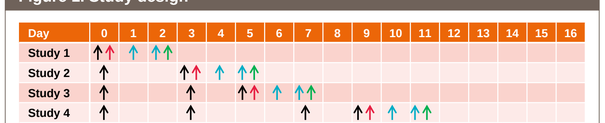

Black arrows represent mAb injection, red arrows represent ^{89}Zr–anti-CD8 minibody injection, blue arrows represent PET/CT imaging, green arrows represent *ex vivo* assessment.

Results

Figure 2. Antitumor activity in a syngeneic murine model of breast cancer (EMT6)

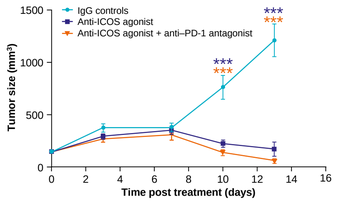

Tumor size was measured in study 5 at Day 0, 3, 7, 10, and 13. Tumor size was significantly lower at Day 10 and 13 post treatment in both anti-ICOS agonist (n=12) and anti-ICOS agonist + anti–PD-1 antagonist (n=12) treatment groups, relative to IgG control group (n=12). Overall, 4 and 9 mice were clearing tumors by end of study (Day 16) in the anti-ICOS agonist and anti-ICOS agonist + anti–PD-1 antagonist treatment groups, respectively. ***P<0.001 (two-way ANCOVA model accounting for heterogeneity of variance and with animal as a random effect).

Figure 3. Representative *in vivo* PET/CT and IHC images

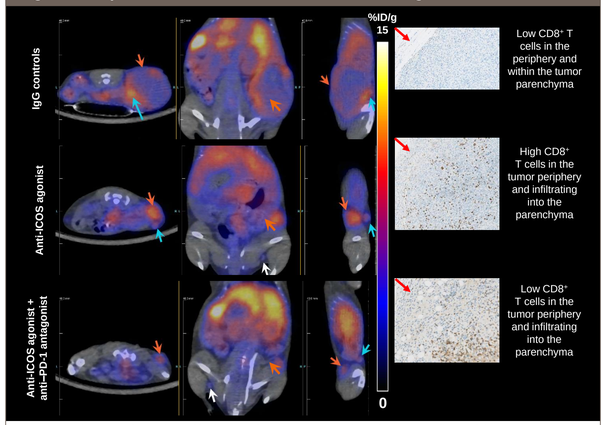

Representative co-registered PET/CT images (study 5 on Day 15), and corresponding IHC images.
Upper panel: A mouse receiving IgG controls showed heterogenous ^{89}Zr–anti-CD8 minibody uptake in the tumor with limited uptake in the tumor core; IHC showed low CD8$^+$ T-cell infiltration in the parenchyma.
Middle panel: A mouse receiving anti-ICOS agonist mAb showed high and homogenous minibody uptake in a small tumor; IHC showed high CD8$^+$ T-cell infiltration in the tumor.
Lower panel: A mouse receiving anti-ICOS agonist + anti–PD-1 antagonist mAbs showed moderate homogenous minibody uptake in a small tumor and in the TDLN; IHC showed low CD8$^+$ T-cell infiltration in the tumor periphery and infiltrating into the tumor parenchyma.
Orange arrows indicate tumor, blue arrows indicates TDLN, white arrow indicates non-draining lymph node, red arrow indicates direction from periphery to the tumor core.

Figure 4. ^{89}Zr–anti-CD8 minibody uptake in TDLN

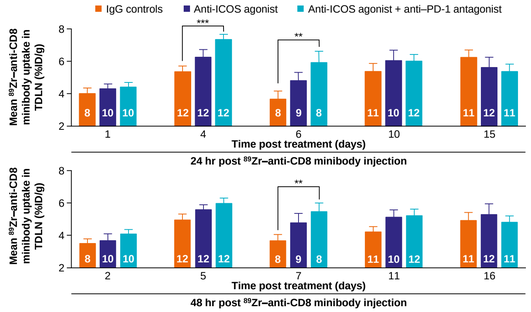

In vivo ^{89}Zr–anti-CD8 minibody uptake in TDLN following treatment with anti-ICOS agonist mAb or anti-ICOS agonist + anti–PD-1 antagonist mAbs, as measured using PET/CT imaging at (**upper panel**) 24 hr or (**lower panel**) 48 hr post minibody injection. Minibody uptake in TDLN was significantly higher in the anti-ICOS agonist + anti–PD-1 antagonist treatment group on Days 4, 6, and 7, compared to IgG control group. White numbers represent the number of TDLN (mice) per group. **P<0.01, ***P<0.001 (two-way ANOVA with animal as a random effect).

Figure 5. ^{89}Zr–anti-CD8 minibody uptake in tumor

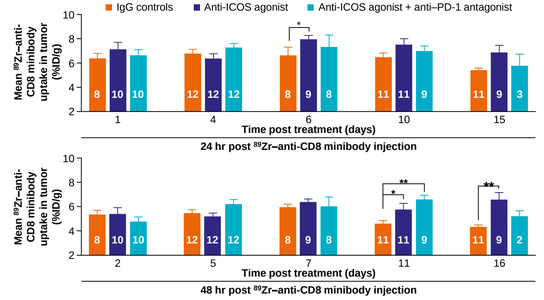

In vivo mean ^{89}Zr–anti-CD8 minibody uptake in tumor following treatment with anti-ICOS agonist mAb or anti-ICOS agonist + anti–PD-1 antagonist mAbs, as measured using PET/CT imaging at (**upper panel**) 24 hr or (**lower panel**) 48 hr post minibody injection. Minibody uptake in the tumor was significantly higher in the anti-ICOS agonist treatment group on Day 6, 11, and 16, and in the anti-ICOS agonist + anti–PD-1 antagonist treatment group on Day 11, compared to IgG control group. White numbers represent the number of tumors (mice with measurable tumor) per group. *P<0.05, **P<0.01 (two-way ANOVA with animal as a random effect).

Figure 6. Hyperion images showing representative phenotypes

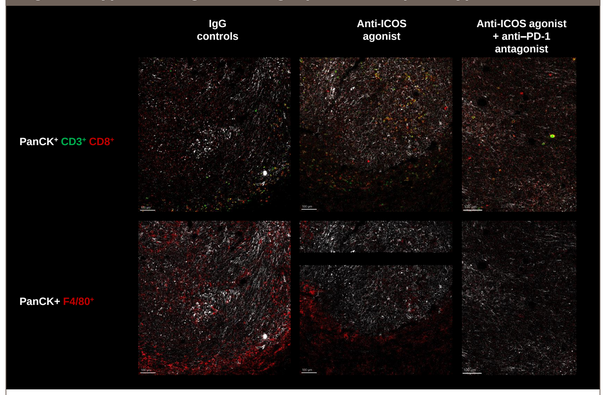

Upper panel: Pan cytokeratin$^+$ (PanCK; white, tumor marker) and CD3$^+$CD8$^+$ (green+red=yellow, cytotoxic T cells). In the IgG controls-administered sample, cytotoxic T cells were observed in the peripheral region of the tumor; in the anti-ICOS agonist-treated sample, cytotoxic T cells infiltrated into the tumor; in the anti-ICOS agonist + anti–PD-1 antagonist-treated sample, the tumor was resolved with spreading PanCK$^+$ cells accompanied by a few cytotoxic T cells.
Lower panel: PanCK$^+$ (white, tumor marker) and F4/80$^+$ (red, macrophages). In the IgG controls-administered sample, high tumor-macrophage interaction was prevalent in the tumor; in the anti-ICOS agonist-treated sample, tumor cells showed higher interaction with cytotoxic T cells when compared with macrophages, whereas macrophages were found mainly in the peripheral region; in the anti-ICOS agonist + anti–PD-1 antagonist-treated sample, PanCK$^+$ tumor cells were low in number and the proliferative cells were admixed with macrophages and cytotoxic T cells.
Analysis was performed on limited number of samples (n=2 per group, and one region of interest per sample).

Figure 7. Radiomics feature analysis

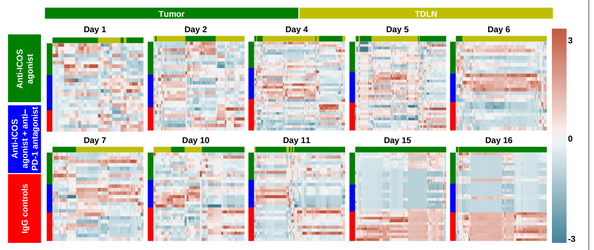

Cluster heatmaps for IgG control, anti-ICOS agonist, and anti-ICOS agonist + anti–PD-1 antagonist treatment groups, with 3D radiomic features extracted from PET/CT images. The anti-ICOS agonist + anti–PD-1 antagonist group started expressing a different signature when compared to IgG control group as early as Day 4. In early timepoints (Day 4, 5, 6, 7), features from TDLN (light green) distinguish the different treatment groups; the anti-ICOS agonist + anti–PD-1 antagonist group expressed higher values, the anti-ICOS agonist group expressed high and low values, whereas IgG control group expressed lower values. In later timepoints (Day 11, 15, 16), most features from the tumor (dark green) in anti-ICOS agonist and anti-ICOS agonist + anti–PD-1 antagonist groups expressed lower values, whereas IgG control group expressed higher values.

Conclusions

- These data demonstrate for the first time that treatment of tumor-bearing mice with an anti-ICOS agonist mAb, alone or in combination with PD-1 blockade, can increase CD8$^+$ T-cell infiltration into tumors and TDLN, and is correlated with reduced tumor burden.
- Whereas anti-ICOS agonist mAb demonstrated a similar therapeutic effect on CD8$^+$ T-cell kinetics in the tumor when used alone and in combination with PD-1 blockade, the combination treatment resulted in significantly earlier uptake of ^{89}Zr–anti-CD8 minibody in the TDLN compared to ICOS agonism alone.
- Notably, radiomics features predicted treatment effects on CD8$^+$ T-cell infiltration earlier than detection of ^{89}Zr–anti-CD8 minibody uptake in the tumor and TDLN.
- The presented data support the translational imaging method shown as a useful tool for non-invasively monitoring CD8$^+$ T-cell responses to immunotherapies, and for understanding the temporal relationship between CD8$^+$ T-cell flux in the tumor and in TDLN.
- These data support the ongoing evaluation of feladilimab in pivotal oncology clinical trials.[8,9]

References

1. Burmeister Y, et al. *J Immunol* 2008;180:774–82;
2. Hutloff A, et al. *Nature* 1999;397:263–66;
3. Mayes P, et al. *Nat Rev Drug Discov* 2018;17:509–27;
4. Brett S. et al. *Ann Oncol* 2018;29(suppl_8):viii649–69;
5. Angevin E, et al. *J Clin Oncol* 2020;38(15_suppl):6517;
6. Massarelli E, et al. ASCO 2020 poster presentation: abstract 6544;
7. Hansen A, et al. *Ann Oncol* 2018;29(suppl_8):viii404;
8. Angevin E, et al. *J Clin Oncol* 2020;38(suppl_15):6517;
9. ClinicalTrials.gov. Available at https://clinicaltrials.gov/ct2/show/NCT04428333. Last Accessed: February 12, 2020;
10. Giesen C, et al. *Nat Methods* 2014;11:417–22.

Acknowledgements

- **Disclosures**: **HA**, **S-HC**, **MBi**, **MR**, **TS**, **BH**, **SM**, **AG**, **CY-H**, **MD**, **FX**, **RG**, **CBH**, **SB**, **AN**, **JDW**, and **BMJ** are employees of GSK; **IW** is an employee of ImaginAb; **MBallas** is an employee of, has held leadership roles at, has received research funding from, and received travel/accommodations/expenses from GSK, holds stocks/shares in GSK, Bristol Myers Squibb, and Moderna, has patents/royalties/other intellectual property in GSK and AstraZeneca, and an immediate family member has a relationship not otherwise specified with Abbvie; **AH** is an employee of GSK, has held leadership roles at Imugene and TCR2 Therapeutics, has received travel/accommodation/expenses from, and holds stocks/other ownership interests in GSK, Imugene, and TCR2 Therapeutics.
- This work was funded by GSK. Editorial support (in the form of copy editing) was provided by Victoria Hunter, MSc, at Fishawack Indicia Ltd, UK, and was funded by GSK.

Presenting author: hasan.5.alsaid@gsk.com

Presented at the AACR Annual Meeting, Virtual Format, Week 1, April 10–15, 2021